SMITHSONIAN INSTITUTION
ASTROPHYSICAL OBSERVATORY

Research in Space Science

SPECIAL REPORT

Number 218

GEOMAGNETIC PERTURBATIONS AND UPPER-ATMOSPHERE HEATING

L. G. Jacchia, J. Slowey, and F. Verniani

August 22, 1966

CAMBRIDGE, MASSACHUSETTS 02138

SAO Special Report No. 218

GEOMAGNETIC PERTURBATIONS AND UPPER-ATMOSPHERE HEATING

L. G. Jacchia, J. Slowey, and F. Verniani

Smithsonian Institution
Astrophysical Observatory
Cambridge, Massachusetts 02138

7-66-10

TABLE OF CONTENTS

LIST OF ILLUSTRATIONS

LIST OF TABLES

ABSTRACT

The density variations that accompany geomagnetic disturbances have been studied by analyzing the drag of three satellites with high orbital inclination (Injun 3, Explorer 19, and Explorer 24) and one with moderate inclination (Explorer 17). The average time delay between the peak of the geomagnetic perturbation and that of the atmosphere is 6.7 ± 0.3 hours. While there seems to be no significant dependence of the time delay on the intensity of the perturbation and on the geographic location with respect to the sun, there appears to be some dependence on latitude. For latitudes greater than 55° (average: 65°) the mean time delay is 5.8 ± 0.5 hours, and for latitudes smaller than 55° (average: 25°) it is 7.2 ± 0.3 hours. All three high-inclination satellites give consistently smaller delay times at high latitudes.

The observed density changes are interpreted as caused by changes in temperature. For smaller perturbations ($K_p < 5$) the temperature T shows a nearly linear dependence on K_p, and for latitudes lower than 55° the rate of change $\Delta T/\Delta K_p$ is about 28°. For latitudes above 55° (average: 65°) $\Delta T/\Delta K_p$ seems to be about 15 to 25 percent greater. For more intense disturbances ($K_p \geq 5$), $\Delta T/\Delta K_p$ is systematically larger, confirming the nonlinearity of the relation between T and K_p, when considered over its total range; there is also a good indication that some atmospheric perturbations are enhanced in the auroral zones more than others.

GEOMAGNETIC PERTURBATIONS AND UPPER-ATMOSPHERE HEATING[1]

L. G. Jacchia,[2] J. Slowey,[3] and F. Verniani[4]

1. GENERAL

Early drag research on artificial satellites (Jacchia, 1959) established the fact that the temperature and density of the upper atmosphere increase during magnetic storms. Later investigations (Jacchia and Slowey, 1964a, b, c) revealed several interesting details of such atmospheric perturbations, namely:

A. Even the smallest variations in geomagnetic activity are reflected in atmospheric variations. During magnetic storms proper, the temperature variations seem to be related in a near-linear fashion with the planetary geomagnetic index a_p, while during quieter periods the relation is nearly linear with the planetary index K_p, which is the logarithmic counterpart of a_p. Thus, the relation between the temperature and any one of the two indices is nonlinear. Since the a_p index is proportional to the variations of the magnetic field, we see that the rate of temperature variation per unit field variation, $\Delta T/\Delta a_p$ is greater when a_p is smaller.

---

[1]This work was supported in part by Grant No. NsG 87-60 from the National Aeronautics and Space Administration.

[2]Physicist, Smithsonian Astrophysical Observatory.

[3]Astronomer, Smithsonian Astrophysical Observatory.

[4]Physicist, Smithsonian Astrophysical Observatory and Harvard College Observatory; now at Centro Nazionale per la Fisica dell'Atmosfera e la Meteorologia del CNR, Rome, Italy.

B. Atmospheric perturbations lag behind geomagnetic perturbations by several hours.

C. The temperature increase during a magnetic disturbance is, at least occasionally, enhanced at high latitudes.

The study of transient density fluctuations such as those observed at the time of magnetic storms is rather difficult by the drag-analysis method, owing to the limited resolution it affords. Actually, even the detection of minor perturbations of this type is not an easy task, because the quantity to be determined, the acceleration in the satellite's mean motion, is the second time derivative of the mean anomaly, which when the orbit is known, can be considered to be the basic observational quantity.

The first prerequisite for obtaining derivatives of a function is that the function be smooth. Smoothing formulas cannot be trusted to do a satisfactory job when the observations are unevenly distributed and when we have to deal with sharp inflections in the curve they determine. If we really want to use the observations to the limit of their accuracy, there is no substitute for a curve drawn by hand through a plot of the observed data, with the aid of French curves or the like, no matter how laborious and old-fashioned this procedure may look to a modern researcher used to push-button devices. Wholly automated programs can be used to obtain atmospheric densities with good results for studying variations with characteristic times of several days, weeks, or months; they will fail, however, to do justice to the observations in the case of irregular, short-lived fluctuations — except, perhaps, in the case of satellites with very low perigee heights, for which the drag is so large that a high resolution may be obtained even with cruder methods.

For a statistical investigation aimed at covering both large and small atmospheric perturbations we needed satellites with large atmospheric drag. A high orbital inclination was needed to study the effect of geomagnetic latitude on the perturbations, while a moderately

high eccentricity was necessary to ascribe the drag information to a specific location in the atmosphere. In addition we wanted the satellites to be relatively long-lived, so that each one would provide, if possible, enough data to allow a separate statistical analysis.

This last point needs some amplifying. For any single atmospheric perturbation the amplitude of the density fluctuation varies greatly with height, so that data from one satellite cannot be directly compared with those of another satellite with different perigee height. It is true that when we convert the density variations to temperature variations with a suitable model, we obtain amplitudes that seem to be roughly independent of height (Jacchia, 1965). Nevertheless, some systematic dependence on height must be expected also in the temperature amplitudes, since it is unlikely that the energy dissipation during geomagnetic disturbances has exactly the same height distribution as the one that is implicit in the atmospheric models; moreover, in such short-lived phenomena we must expect considerable departure from the equilibrium conditions of the models.

The four satellites selected for this investigation are listed in Table 1, with their pertinent characteristics. Three of these satellites (Injun 3, Explorer 19, and Explorer 24) meet all the aforementioned conditions. Explorer 17 was included in spite of the somewhat smaller inclination and eccentricity of its orbit, since variations with geomagnetic activity were also recorded by density gauges on this satellite (Newton, Horowitz, and Priester, 1964). In Table 1 A/m is the ratio of the average presentation area of the satellite to its mass, and dP/dt is an approximate value of the average change of period with time. In the next two columns we have given quantities relevant to the plots of residuals in the mean anomaly M, from which the drag was derived. The first of these two quantities, n, is the degree of the power polynomial approximating M, from which the residuals ΔM were computed. The second quantity, τ, is the length of the time interval covered by the individual ΔM plots.

Table 1. Basic data on satellites

Satellite	Perigee height (km)	Apogee height (km)	Incl.	A/m (cm^2/g)	-dP/dt (average)	n	τ (days)	Interval covered by analysis
1962 $\beta\tau$2 (Injun 3)	250	2500	70°3	0.070	4×10^{-6}	5	40	15 Dec. 1962 - 12 Jul. 1965
1963 09 A (Explorer 17)	270	800	57.6	0.036	2×10^{-6}	4	40-50	8 Apr. 1963 - 9 Oct. 1963
1963 53 A (Explorer 19)	615	2300	78.6	13.0	1×10^{-6}	4	40-70	27 Dec. 1963 - 24 Aug. 1965
1964 76 A (Explorer 24)	545	2400	81.4	12.2	2×10^{-6}	4-5	40-70	27 Nov. 1964 - 26 Jul. 1965

2. TIME LAG

As we mentioned in the previous section, to obtain the secular accelerations of satellites we used curves drawn on plots of residuals ΔM from low-power polynomials fitted to the observed mean anomalies. The polynomial takes care of most of the systematic part of the accelerations; all the remaining fluctuations with short characteristic times (1/2 day to 2 days) are related to magnetic storms. As a consequence of atmospheric heating during the storm, the drag of a satellite rises to a maximum and then relapses to a more normal value. Since the drag is very nearly proportional to the second time derivative of the mean anomaly, it should be clear that any peak in the drag must result in a dip in the ΔM curve (see Figure 1).

To compute densities and temperatures we cannot make the interval of differentiation in the ΔM's too small, lest we obtain results of marginal significance. If, however, we are interested only in determining the time at which the perturbation reached its maximum, we can afford to decrease the interval of differentiation. For this reason we did not use densities or temperatures in the determination of the time lag between magnetic and atmospheric disturbances, but rather went back to the original ΔM curves, which were read off for differentiation at 0.2-day intervals around each dip (in the case of very sharp dips the time of minimum could easily have been read off by eye on the curve without any loss of accuracy). The polynomial part of the drag can be entirely neglected in these time determinations, because it accounts only for slow drag variations, with characteristic times of the order of $2\tau/n$ (see Table 1), i.e., of a few weeks.

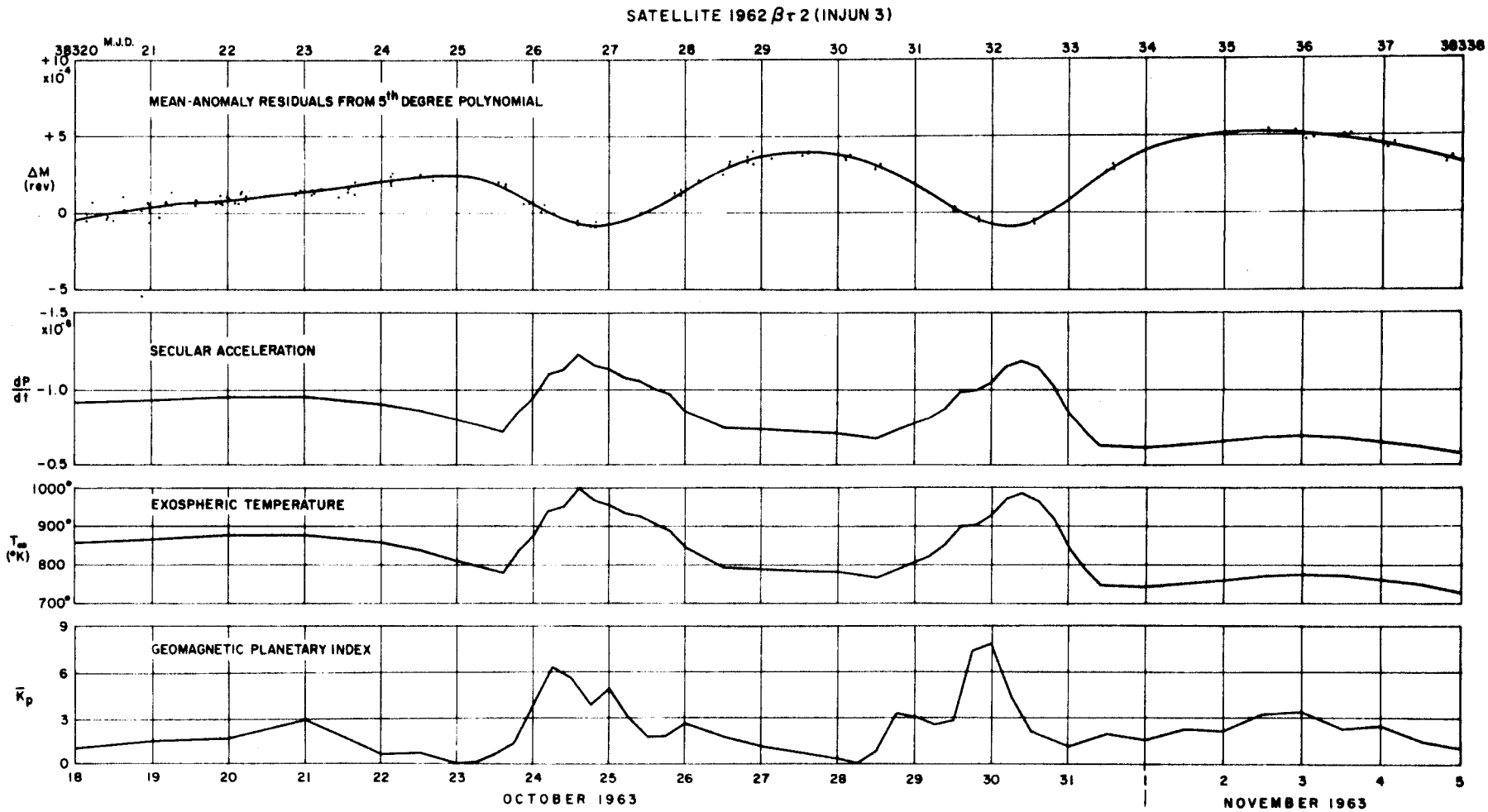

Figure 1. The effect of two moderate geomagnetic storms on the motion of the Injun 3 satellite, and the derived variations of atmospheric density and temperature. The bottom section is a plot of the geomagnetic planetary index K_p, smoothed to match the variable resolution of the satellite data. The lag of the density and temperature curves with respect to the $\overline{K}_p$ curve can be noticed at a glance. MJD in the abscissa is the Modified Julian Day (Julian Day minus 2 400 000.5).

The time of maximum of the atmospheric perturbation was derived by differentiation to the nearest tenth of a day and then compared with the maximum of the magnetic disturbance, read off with the same degree of accuracy from a plot of the K_p index. Obviously not all disturbances are equally suitable for determining the time lag. The ideal case is that of a sharp, single-peaked magnetic disturbance, with a corresponding sharp dip in the ΔM curve, well covered by observations with small dispersion around the curve. A favorable case such as this is rated a weight 3 in our memory-based scale. It was more common, however, to find that either the minimum of the ΔM curve or the maximum of the K_p curve could not be so accurately located, in which case a lower weight was assigned to the lag determination. Many geomagnetic disturbances, even important ones, could not be used at all for determining the time lag on account of their irregular character. Other pronounced disturbances, notably those belonging to the series that recurred from the 5th to the 9th day of each solar rotation from August 1962 to mid-1964, were generally too prolonged for the determination of time differences.

Table 2 gives all the geomagnetic perturbations used for the determination of the time lag Δt and of the ratio $\Delta T/\Delta K_p$, listed separately for each satellite. The time is given in Modified Julian Days (MJD = Julian Day minus 2 400 000.5). Since the criteria for determining the time lag differ considerably from those for deriving the magnitude of the disturbance, we had to use two systems of weights, w_1 for Δt and w_2 for $\Delta T/\Delta K_p$. The maximum observed value of the 3-hourly K_p index during the disturbance is K_{pmax} (more about this quantity and about ΔT will be found in Section 3). The observed range in K_p is $\Delta \bar{K}_p$, smoothed to match the time resolutions appropriate to the individual satellite. Also listed are the geographic latitude ϕ, the difference between the right ascension of the satellite's perigee α_π and that of the sun $\alpha_\odot$, as well as the angular distance ψ between the satellite's perigee and the sun.

Table 2. Basic data on individually observed atmospheric perturbations connected with geomagnetic disturbances.

a) Injun 3

MJD	Δt	w_1	K_{pmax}	ΔT (°K)	$\Delta\overline{K}_p$	$\Delta T/\Delta\overline{K}_p$	w_2	ϕ	$a_\pi - a_\odot$	ψ
38060.2	0.3	2	5.7*	290	5.2	55.8	2	70°	287°	100°
070.2	0.4	1	5.7*	210	4.7	44.7	2	70	229	117
080.9	-	-	3.7	55	1.3	42.3	3	64	170	126
089.2	-	-	4.0	45	1.4	32.1	2	57	133	118
098.7	-	-	6.3*	95	4.5	21.1	1	50	105	103
107.2	-	-	2.7	70	1.5	46.7	2	41	73	78
111.5	0.4	1	4.0	35	1.2	29.2	1	37	61	66
124.2	0.2	2	5.7	70	4.4	15.9	1	24	22	28
134.1	-	-	4.7	90	3.5	25.7	2	14	353	9
187.1	0.4	2	7.0*	155	6.0	25.8	2	-41	187	161
198.8	0.4	1	5.0	75	2.5	30.0	2	-52	145	141
206.1	0.2	2	5.7*	125	4.6	27.2	2	-59	116	123
215.5	-	-	5.7	95	4.0	23.8	1	-66	74	104
227.3	-	-	3.7	75	2.1	35.7	1	-70	9	92
231.5	-	-	5.3	45	2.5	18.0	1	-70	342	91
240.4	0.3	1	5.0	130	3.8	34.2	1	-66	294	98
261.1	-	-	7.0*	135	5.0	27.0	1	-49	208	137
269.5	0.4	1	5.3	40	1.9	21.0	1	-41	179	149
283.8	-	-	5.0	85	1.7	50.0	1	-26	132	129
286.4	0.2	3	7.0*	165	6.1	27.0	3	-24	127	125
294.7	0.3	1	8.7*	200	5.4	37.0	2	-15	101	101
314.4	0.3	1	5.7	125	3.0	41.7	2	6	41	43
316.3	0.4	1	4.7	30	1.0	30.0	1	8	36	39
326.3	0.3	2	7.3*	225	6.4	35.2	3	18	5	30
331.9	0.4	2	8.0*	220	6.8	32.4	3	24	348	39
335.7	-	-	5.0	35	2.0	17.5	2	28	336	49
341.0	-	-	6.0	80	4.0	20.0	3	33	320	63
350.7	-	-	4.7	50	2.8	17.9	2	44	285	93
358.0	-	-	5.0	75	3.5	21.4	2	50	261	111
363.5	0.1	1	5.7	100	1.5	66.7	1	56	238	126

Table 2 (Cont.)

a) Injun 3

MJD	Δt	w_1	K_{pmax}	ΔT (°K)	$\Delta\bar{K}_p$	$\Delta T/\Delta\bar{K}_p$	w_2	ϕ	$\alpha_\pi - \alpha_\odot$	ψ
38366.3	-	-	5.7	100	2.7	37.0	1	60°	217°	134°
377.7	-	-	3.7	70	2.2	31.8	1	67	174	136
383.3	-	-	4.7	75	2.3	32.6	1	69	140	128
392.5	-	-	4.0	60	2.4	25.0	1	70	88	111
396.4	-	-	6.7*	135	5.0	27.0	2	69	62	102
404.1	0.2	1	4.7	55	2.5	22.0	2	64	23	88
410.7	0.2	2	5.0	115	4.0	28.8	2	59	352	80
419.5	-	-	4.7	50	2.0	25.0	1	51	318	79
423.3	0.5	1	4.0	60	2.6	23.1	2	47	303	83
431.3	0.2	1	5.3	80	2.8	28.6	2	40	276	95
434.0	-	-	5.7	20	1.0	20.0	1	37	267	101
438.3	0.1	1	5.0	75	3.7	20.3	2	32	252	112
486.9	0.4	1	7.3*	160	4.5	35.6	2	-19	101	102
496.6	-	-	4.7	20	2.5	8.0	1	-30	70	77
503.6	-	-	5.0	45	2.0	22.5	1	-37	48	66
513.0	0.2	1	5.3	80	4.0	20.0	2	-47	16	63
516.0	0.2	1	6.0	65	3.0	21.7	2	-50	5	65
526.1	0.1	2	5.3*	255	4.8	53.1	3	-59	326	82
529.5	-	-	6.0	40	4.0	10.0	1	-62	309	90
540.4	-	-	6.3	75	3.8	19.7	2	-69	255	116
556.3	0.4	1	6.7	155	4.5	34.4	2	-68	159	133
566.6	-	-	5.0	60	2.4	25.0	1	-60	109	119
580.0	-	-	4.3	50	2.2	22.7	1	-48	56	87
584.0	-	-	4.7	70	3.0	23.3	1	-43	39	75
593.7	-	-	5.7	55	3.5	15.7	1	-33	6	55
605.8	-	-	4.7	50	2.4	20.8	2	-20	325	52
611.2	0.1	2	6.3	65	3.6	18.1	2	-15	310	59
618.8	0.5	1	4.7	45	2.9	15.5	3	- 7	286	76
680.5	-	-	4.3	25	3.3	7.6	-	58	83	93
687.6	-	-	4.7	60	3.3	18.2	1	64	52	84

Table 2 (cont.)

a) Injun 3

MJD	Δt	w_1	K_{pmax}	ΔT (°K)	$\Delta\bar{K}_p$	$\Delta T/\Delta\bar{K}_p$	w_2	ϕ	$a_\pi - a_\odot$	ψ
38694.4	0.2	2	5.3	115	4.0	28.8	2	68°	17°	82°
701.0	0.3	3	4.7	125	4.0	31.2	3	70	338	86
704.8	-	-	3.3	20	1.1	18.2	1	70	318	91
708.2	0.2	1	4.7	165	4.0	41.2	2	69	294	98
714.9	-	-	4.3	90	3.0	30.0	2	66	256	113
722.4	0.3	3	4.7	135	3.9	34.6	3	60	220	131
726.2	-	-	3.3	60	2.1	28.6	1	57	204	140
736.8	-	-	3.3	15	2.3	6.5	-	47	162	69
745.8	-	-	5.3	45	2.8	16.1	1	38	130	135
763.1	-	-	4.0	75	1.5	50.0	1	18	68	78
768.4	0.3	1	4.3	70	2.1	33.3	1	12	51	61
773.0	0.3	1	4.3	30	2.5	12.0	1	8	37	46
777.6	-	-	3.7	20	1.5	13.3	1	3	22	32
782.5	0.3	1	5.7	90	3.0	30.0	1	- 3	6	18
790.0	-	-	2.7	45	1.0	45.0	2	-11	343	18
798.3	0.5	1	5.7*	135	3.0	45.0	1	-20	314	45
799.9	-	-	5.3	45	2.2	20.5	1	-22	310	48
805.4	-	-	3.7	20	1.5	13.3	1	-28	290	66
814.7	-	-	5.0	20	1.5	13.3	1	-38	260	92
823.2	-	-	6.0	65	2.3	28.3	1	-47	229	111
833.5	-	-	3.3	50	1.5	33.3	1	-57	190	120
843.0	-	-	5.0	90	2.6	34.6	2	-65	150	113
860.0	-	-	4.0	45	1.5	30.0	2	-69	39	82
868.3	0.3	1	7.7*	210	6.5	32.3	3	-66	2	77
986.6	-	-	5.3	60	1.7	35.3	1	-39	247	120
903.0	-	-	2.3	45	0.9	50.0	1	-32	223	140
927.7	0.2	1	7.0*	220	4.7	46.8	2	- 5	143	140
936.7	-	-	4.0	70	1.8	38.9	1	5	113	109

Table 2 (cont.)

b) Explorer 17

MJD	Δt	w_1	K_{pmax}	ΔT (°K)	$\Delta\bar{K}_p$	$\Delta T/\Delta\bar{K}_p$	w_2	ϕ	$a_\pi - a_\odot$	ψ
38134.0	0.2	1	4.7	180	3.2	56.2	2	52°	106°	92°
138.0	-	-	4.3	35	0.8	43.8	1	55	94	83
150.0			6.3*	120	4.5	26.7	2	57	69	66
160.1	-	-	4.3	55	1.5	36.7	2	53	46	50
178.2	0.3	1	5.7	60	3.5	17.1	2	35	349	17
187.1	0.4	1	7.0*	225	5.7	39.5	3	24	313	43
198.8	0.0	1	5.0	90	3.2	28.1	3	9	267	89
206.1	0.2	2	5.7*	140	4.5	31.1	3	- 1	237	121
216.2	-	-	5.7*	145	4.5	32.2	2	-15	195	164
219.1	-	-	4.0	20	0.7	28.6	1	-19	182	176
227.3	-	-	3.7	95	1.7	55.9	2	-30	149	151
231.5	0.3	2	5.3	190	4.0	47.5	3	-35	134	138
234.0	0.1	1	5.3*	80	2.9	27.6	2	-38	126	130
240.4	-	-	5.0	50	2.7	18.5	2	-45	103	112
269.8	-	-	5.3	25	1.0	25.0	1	-54	38	71
284.0	-	-	5.0	45	1.7	26.5	1	-41	358	45
286.3	-	-	7.0*	130	4.5	28.9	1	-38	348	42
289.4	-	-	6.7*	30	0.7	42.9	1	-33	338	41
295.0	-	-	8.7*	165	4.2	39.3	1	-26	317	49
310.0	-	-	4.7	105	2.4	43.8	1	- 5	256	103

Table 2 (cont.)

c) Explorer 19

MJD	Δt	w_1	K_{pmax}	ΔT (°K)	$\Delta\bar{K}_p$	$\Delta T/\Delta\bar{K}_p$	w_2	ϕ	$a_\pi - a_\odot$	ψ
38396.3	0.3	1	6.7	60	3.0	20.0	2	45°	311°	81°
403.0	-	-	4.7	25	1.3	19.2	1	57	291	97
450.8	-	-	5.7	50	1.4	35.7	1	26	39	52
458.7	0.2	1	6.0	85	4.1	20.7	3	12	21	28
470.0	-	-	3.7	15	1.0	15.0	1	-10	356	9
476.8	-	-	5.7	70	3.5	20.0	2	-23	340	31
486.9	0.2	3	7.3*	70	5.2	13.5	2	-42	316	62
503.6	-	-	5.0	30	2.0	15.0	1	-72	254	105
512.7	-	-	5.3	45	3.5	12.9	1	-77	161	116
516.0	0.2	1	6.0	60	1.8	33.3	1	-74	135	116
526.1	-	-	5.3	35	2.8	12.5	1	-57	90-	105
530.2	-	-	6.0	45	2.5	18.0	1	-48	76	95
540.4	-	-	6.3	30	2.3	13.0	2	-29	49	69
556.3	0.2	3	6.7	135	4.0	33.8	2	1	11	25
566.6	0.1	1	5.0	90	2.0	45.0	2	20	347	13
579.8	0.2	1	4.3	-	-	-	-	45	313	44
593.7	-	-	5.7	215	3.4	63.2	1	70	261	73
611.2	0.3	2	6.3	-	-	-	-	69	114	82
618.8	0.2	1	4.7	95	2.2	43.2	2	56	85	75
633.1	-	-	3.3	105	1.5	70.0	2	29	47	47
639.0	-	-	4.7	55	2.1	26.2	2	18	33	33
645.8	0.2	1	5.0	135	3.5	38.6	3	5	18	18
654.9	0.2	1	3.7	60	2.3	26.1	2	-12	357	15
660.2	0.5	2	7.7	170	4.0	42.5	1	-23	344	28
666.7	-	-	5.7	80	2.3	34.8	2	-35	329	44
680.4	-	-	4.3	95	1.8	52.8	1	-61	290	74
687.6	-	-	4.7	40	2.0	20.0	2	-73	256	84
694.3	-	-	5.3	140	2.9	48.3	2	-79	189	89
701.0	0.2	1	4.7	80	2.2	36.4	1	-72	131	87
708.2	0.5	1	4.7	50	2.1	23.8	2	-59	98	79

Table 2 (cont.)

c) Explorer 19

MJD	Δt	w_1	K_{pmax}	ΔT (°K)	$\Delta\bar{K}_p$	$\Delta T/\Delta\bar{K}_p$	w_2	ϕ	$\alpha_\pi - \alpha_\odot$	ψ
38714.9	-	-	4.3	90	2.0	45.0	1	-46°	75°	66°
722.4	0.6	1	4.7	65	2.0	32.5	1	-32	56	51
727.0	-	-	3.3	25	1.3	19.2	1	-25	46	42
746.1	-	-	4.7	25	2.4	10.4	1	11	359	35
798.3	0.3	1	5.7	50	1.6	31.2	1	62	97	107
823.2	0.6	1	6.0	40	2.0	20.0	1	15	29	36
832.5	-	-	3.3	25	1.7	14.7	1	- 2	9	9
842.8	-	-	5.0	60	2.6	23.1	2	-22	344	28
859.2	-	-	4.0	45	1.5	30.0	1	-54	301	79
868.3	0.0	2	7.7*	170	5.0	34.0	2	-69	270-	100
885.3	-	-	5.3	30	2.2	13.6	2	-69	121	116
896.6	0.5	1	5.3	55	1.6	34.4	1	-48	79	97
914.8	-	-	4.3	35	1.2	29.2	1	-11	31	45
919.0	-	-	3.7	30	1.5	20.0	1	- 4	21	34
927.7	0.2	3	7.0*	190	6.0	31.7	2	11	2	12
936.7	-	-	4.0	30	1.8	16.7	1	29	340	19
941.9	-	-	4.3	10	1.6	6.2	1	38	327	32
947.2	-	-	4.7	70	2.4	29.2	3	48	313	45
974.6	-	-	3.3	95	1.5	63.3	1	71	124	84
990.8	-	-	6.3	70	2.6	26.9	1	43	70	67

Table 2 (cont.)

d) Explorer 24

MJD	Δt	w_1	K_{pmax}	ΔT (°K)	$\Delta\overline{K}_p$	$\Delta T/\Delta\overline{K}_p$	w_2	ϕ	$\alpha_\pi - \alpha_\odot$	ψ
38789.3	-	-	2.7	40	1.0	40.0	2	18°	25°	44°
798.3	0.6	2	5.7	70	2.8	25.0	1	- 2	5	14
805.4	0.3	1	3.7	-	-	-	-	-16	352	9
806.7	0.3	1	4.0	30	2.0	15.0	1	-19	349	13
812.2	-	-	4.7	35	2.2	15.9	1	-30	338	28
814.8	0.3	1	-	-	-	-	-	-36	332	37
816.1	-	-	5.0	85	2.2	38.6	1	-38	330	40
823.2	0.2	3	6.0	115	3.3	34.8	2	-54	312	61
832.5	-	-	3.3	40	1.7	23.5	1	-73	278	85
842.8	0.3	2	5.0	75	3.0	25.0	2	-78	160	102
844.3	0.2	2	5.0	15	0.8	18.8	1	-76	147	104
868.3	0.3	2	7.7*	195	6.5	30.0	3	-26	74	81
885.3	0.4	2	5.3	45	2.5	18.0	1	10	39	39
889.0	0.2	1	4.3	35	2.2	15.9	1	18	32	30
896.5	0.4	2	5.3	65	1.7	38.2	2	34	16	20
903.0	-	-	2.3	40	1.0	40.0	1	47	2	27
914.8	-	-	4.3	55	1.5	36.7	2	73	320	55
920.0	0.2	1	3.7	35	1.5	23.3	1	80	283	65
927.7	0.4	2	7.0*	265	6.0	44.2	2	76	183	81
936.7	-	-	4.0	95	2.4	39.6	1	58	145	93
947.4	0.5	1	4.7	70	2.4	29.2	3	36	118	98
960.3	-	-	4.0	50	1.7	29.4	1	8	90+	88

The weighted mean of all the observed time lags, pooling all satellites together, is $0^d.28 \pm 0.012$ (s.d.), i.e., $6^h.7 \pm 0.3$ (s.d.). We have also given, for comparison, the unweighted mean as well as the medians weighted and unweighted; these are all comprised between $0^d.26$ and $0^d.30$. Thus the time lag turns out to be a little greater than the value of 5 hours derived by Jacchia and Slowey (1964a) and by Roemer (1966) from Explorer 9 drag data alone. There is no clear indication of any variation of the time lag with height in the 250- to 550-km region covered by the four satellites. When the geomagnetic disturbances are divided into two intensity groups, with $\overline{K}_p = 5$ as the dividing limit, we find a lag of $0^d.29 \pm 0.01$ (s.d.) for the low-intensity group and $0^d.26 \pm 0.02$ for the larger perturbations; the difference does not appear to be really significant. The distribution of the observed time lag is shown in Figure 2.

A significant difference is found between the time lag at high and at low latitudes, as can be seen by a comparison of the results for the two groups divided by $|\phi| = 55°$. Geographic, rather than geomagnetic, latitudes have been used, because the rotation of the earth under the perigee point of the satellite tends to blur the distinction between the two; an analysis using geomagnetic latitudes was also made and gave practically identical results. The mean time lag for $|\phi| < 55°$ is $0^d.30 \pm 0.01$ (s.d.) and that for $|\phi| \geq 55°$ is $0^d.24 \pm 0.02$ (s.d.). While the difference between the two values is only twice the sum of the standard deviations, it is significant that each of three satellites (no high-latitude data came from Explorer 17) gave a smaller time lag at high latitudes. The mean latitude of the first group is 25° ; that of the second, 67°. The trend is confirmed when we divide the data into three latitude groups (Table 3c). Assuming a linear relation between Δt and $|\phi|$, we obtain by least squares from all four satellites:

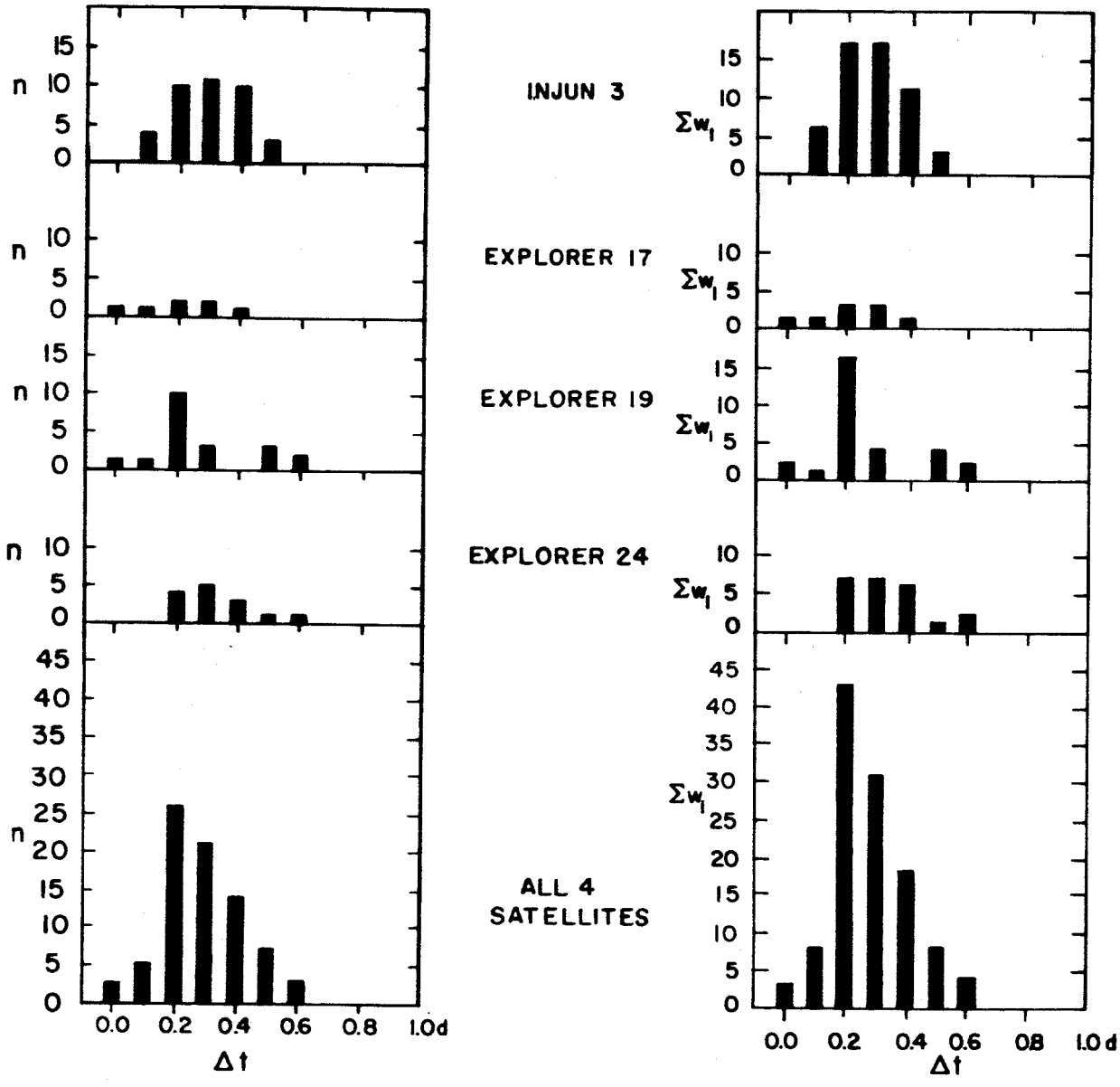

Figure 2. Unweighted (left) and weighted distribution of the observed time differences Δt, between the peak of geomagnetic disturbances and the corresponding atmospheric disturbances.

Table 3. Time lag of atmospheric perturbations behind magnetic storms. Weighted means.

a) Time difference Δt between geomagnetic and atmospheric disturbances

Satellite	Weighted mean ± s. d.	Unweighted mean ± s. d.	Median (weighted)	Median (unweighted)	n
Injun 3	$0^d.28 \pm 0.03$	$0^d.29 \pm 0.04$	$0^d.28$	0.30	54
Explorer 17	0.22 ± 0.04	0.21 ± 0.05	0.25	0.25	9
Explorer 19	0.27 ± 0.03	0.28 ± 0.04	0.23	0.23	29
Explorer 24	0.33 ± 0.03	0.33 ± 0.03	0.32	0.32	23
All satellites	0.28 ± 0.012	0.30 ± 0.02	0.26	0.28	115

b) Weighted means of Δt divided into two groups of geographic latitude

	$\lvert\phi\rvert < 55°$			$\lvert\phi\rvert \geq 55°$		
Satellite	$\overline{\Delta t} \pm$ s. d.	$\lvert\overline{\phi}\rvert$	n	$\overline{\Delta t} \pm$ s. d.	$\lvert\overline{\phi}\rvert$	n
Injun 3	$0^d.31 \pm 0.02$	25°	31	$0^d.23 \pm 0.03$	64°	23
Explorer 17	0.22 ± 0.04	33	9	—	—	—
Explorer 19	0.28 ± 0.04	22	20	0.22 ± 0.05	67	9
Explorer 24	0.35 ± 0.03	27	16	0.29 ± 0.03	77	7
All satellites	0.30 ± 0.01	25	76	0.24 ± 0.02	67	39

Table 3 (cont.)

c) Weighted means of Δt divided into three groups of geographic latitude

	$0° \leq \lvert\phi\rvert \leq 29°$			$30° \leq \lvert\phi\rvert \leq 59°$			$\lvert\phi\rvert \geq 60°$		
	$\overline{\Delta t} \pm$ s.d.	$\overline{\lvert\phi\rvert}$	n	$\overline{\Delta t} \pm$ s.d.	$\overline{\lvert\phi\rvert}$	n	$\overline{\Delta t} \pm$ s.d.	$\overline{\lvert\phi\rvert}$	n
All satellites	$0^d.29 \pm 0.02$	14°	47	$0^d.28 \pm 0.02$	44°	38	$0^d.26 \pm 0.02$	70°	30

d) Weighted means of Δt divided into two groups according to the maximum smoothed value of K_p

	$\overline{K}_{pmax} < 5$		$\overline{K}_{pmax} \geq 5$	
Satellite	$\overline{\Delta t} \pm$ s.d.	n	$\overline{\Delta t} \pm$ s.d.	n
Injun 3	$0^d.27 \pm 0.02$	33	$0^d.29 \pm 0.02$	21
Explorer 17	0.22 ± 0.06	5	0.22 ± 0.06	4
Explorer 19	0.31 ± 0.03	21	0.15 ± 0.10	8
Explorer 24	0.33 ± 0.03	19	0.35 ± 0.03	4
All satellites	0.29 ± 0.01	78	0.26 ± 0.02	37

$$\Delta t = 0.308 - 0.00066\,|\phi| \quad .$$

$$\text{s.d.} \pm 0.018 \pm 0.00040 \quad .$$

This equation gives a difference of only $0^d.03$ between the values of Δt at $|\phi| = 25°$ and $|\phi| = 67°$, instead of the difference of $0^d.06$ found from the division into two groups. The average of the two differences is close enough to 1 hour so we can say that the most acceptable values for the time lag are 7 hours at low latitudes and 6 hours at high latitudes.

From an analysis of 11 low-altitude Agena satellites (perigee heights between 160 and 210 km), DeVries, Friday, and Jones (1966) have found a much stronger dependence of the time lag on latitude: from near-zero around $|\phi| = 75°$ to about 17 hours at $|\phi| = 30°$. Our data seem to preclude such a wide range. While it is true that their satellites have somewhat lower perigee heights, it does not stand to reason that the small difference might account for the discrepancy. It may be relevant to note that all the Agena satellites had very low orbital eccentricities — between 0.013 and 0.027 — a fact that makes it difficult to assign a latitude to a drag observation.

3. HEATING

While earlier satellite-drag data seemed to indicate that the temperature increase ΔT that accompanies a magnetic storm is proportional to the observed increase Δa_p in the 3-hourly planetary a_p index (Jacchia and Slowey, 1964a), later data showed that for moderate and small perturbations ΔT is more nearly proportional to the increase ΔK_p in the 3-hourly K_p index (Jacchia and Slowey, 1964c; Newton et al., 1964). Since the majority of the perturbations listed in Table 2 are of the moderate-to-small variety, we used the variations in the K_p index for comparison with the observed values of ΔT. As we mentioned in Section 2, $\Delta\overline{K}_p$ in Table 2 is the observed range in K_p, smoothed to match the time resolution appropriate to the individual satellite.

In our analysis we divided the geomagnetic perturbations into two intensity groups. In the first group we included all perturbations in which the smoothed K_p index reached a maximum value $\overline{K}_{pmax}$ smaller than 5; the larger perturbations, with $\overline{K}_{pmax} \geq 5$, fell into the second group. The value K_{pmax} listed in Table 2 is the largest value of K_p actually observed during the perturbation. An asterisk signifies that the maximum of the smoothed K_p curve, $\overline{K}_{pmax}$, was greater than 5.

Results relative to the ratio $\Delta T/\Delta\overline{K}_p$ are shown in Table 4. Jacchia's (1965) atmospheric models were used to transform densities into temperatures. As we mentioned in Section 1, the atmospheric models cannot be expected to do a perfect job in operating this transformation, and for this reason we must anticipate the possibility of systematic differences in

Table 4. Ratio of temperature variation ΔT to variation in $\overline{K}_p$. Weighted means. ($\overline{K}_p$ is the geomagnetic planetary index K_p to match the resolution in T.)

a) Data divided according to latitude and intensity groups

	$\lvert\phi\rvert < 55°$				$\lvert\phi\rvert \geq 55°$			
	$\overline{K}_{pmax} < 5$		$\overline{K}_{pmax} \geq 5$		$\overline{K}_{pmax} < 5$		$\overline{K}_{pmax} \geq 5$	
Satellite	$\Delta T/\Delta\overline{K}_p \pm$ s.d.	n	$\Delta T/\Delta\overline{K}_p \pm$ s.d.	n	$\Delta T/\Delta\overline{K}_p \pm$ s.d.	n	$\Delta T/\Delta\overline{K}_p \pm$ s.d.	n
Injun 3	25°.3 ± 1°.6	42	33°.4 ± 2°.3	10	31°.0 ± 1°.7	28	40°.4 ± 5°.2	6
Explorer 17	36.0 ± 4.4	11	34.0 ± 2.1	7	43.8	1	26.7	1
Explorer 19	28.4 ± 2.4	30	22.6 ± 9.1	2	31.9 ± 4.4	15	34.0	1
Explorer 24	30.1 ± 2.7	12	30.0	1	28.6 ± 3.2	6	44.2	1
All satellites	28.3 ± 1.3	95	32.3 ± 1.6	20	31.2 ± 1.6	50	38.8 ± 14.2	9

b) Smaller perturbations ($\overline{K}_{pmax} < 5$) divided according to geographic latitude and sun-angle groups

	$\lvert\phi\rvert < 55°$				$\lvert\phi\rvert \geq 55°$			
	Day (6 am to 6 pm LST)		Night (6 pm to 6 am LST)		Day (6 am to 6 pm LST)		Night (6 pm to 6 am LST)	
Satellite	$\Delta T/\Delta\overline{K}_p \pm$ s.d.	n	$\Delta T/\Delta\overline{K}_p \pm$ s.d.	n	$\Delta T/\Delta\overline{K}_p \pm$ s.d.	n	$\Delta T/\Delta\overline{K}_p \pm$ s.d.	n
Injun 3	24°.5 ± 1°.9	30	27°.8 ± 3°.3	12	27°.5 ± 2°.1	14	34°.2 ± 2°.5	14
Explorer 17	26.5 ± 4.6	4	40.0 ± 5.7	7	–	0	43.8	1
Explorer 19	28.4 ± 2.4	30	–	0	34.2 ± 8.9	4	31.1 ± 5.3	11
Explorer 24	30.3 ± 3.4	10	29.2 ± 1.7	2	30.0 ± 4.8	3	27.1 ± 5.4	3
All satellites	26.9 ± 1.3	74	33.1 ± 2.9	21	29.0 ± 2.1	21	32.7 ± 2.3	29
	$\psi < 90°$		$\psi > 90°$		$\psi < 90°$		$\psi > 90°$	
Injun 3	24°.6 ± 2°.1	28	26°.8 ± 2°.9	14	27°.6 ± 1°.8	6	32°.3 ± 2°.2	22

c) Larger perturbations ($\overline{K}_{pmax} \geq 5$) divided according to geographic latitude and sun-angle groups

	$\lvert\phi\rvert < 55°$				$\lvert\phi\rvert \geq 55°$			
	Day (6 am to 6 pm LST)		Night (6 pm to 6 am LST)		Day (6 am to 6 pm LST)		Night (6 pm to 6 am LST)	
Satellite	$\Delta T/\Delta\overline{K}_p \pm$ s.d.	n	$\Delta T/\Delta\overline{K}_p \pm$ s.d.	n	$\Delta T/\Delta\overline{K}_p \pm$ s.d.	n	$\Delta T/\Delta\overline{K}_p \pm$ s.d.	n
Injun 3	35°.4 ± 2°.9	3	32°.3 ± 3°.2	7	42°.2 ± 7°.0	4	36°.0 ± 8°.5	2
Explorer 17	38.3 ± 2.4	4	30.4 ± 1.4	3	26.7	1	–	0
Explorer 19	22.6 ± 9.1	2	–	0	–	0	34.0	1
Explorer 24	30.0	1	–	0	–	0	44.2	1
All satellites	32.9 ± 2.6	10	31.6 ± 2.2	10	39.6 ± 6.3	5	37.5 ± 4.3	4
	$\psi < 90°$		$\psi > 90°$		$\psi < 90°$		$\psi > 90°$	
Injun 3	35°.4 ± 2°.9	3	32°.3 ± 3°.2	7	42°.7 ± 10°.4	2	38°.7 ± 7°.0	4

$\Delta T/\Delta\bar{K}_p$ between individual satellites. Another reason for expecting systematic differences is the fact that it is difficult to hit the correct degree of smoothing in K_p appropriate to each satellite and each magnetic storm (as the density increases during the storm, so does the resolution in the drag data). In view of these difficulties it is surprising to see that the systematic differences from one satellite to the next are rather small.

Section a) of Table 4 shows at a glance that

1) $\Delta T/\Delta\bar{K}_p$ is systematically larger at higher latitudes, and
2) $\Delta T/\Delta\bar{K}_p$ is systematically larger when the geomagnetic perturbation is more intense.

In Sections b) and c) (of Table 4) we give means of $\Delta T/\Delta\bar{K}_p$ for two groups divided according to the local solar time (LST) corresponding to the satellite perigee point: the first group comprises all perturbations that peaked between 6 am and 6 pm ("day"), and the second those that peaked between 6 pm and 6 am ("night"). For the Injun 3 satellite we also used a subdivision according to the angular distance ψ of the satellite perigee point from the subsolar point: the first group ("day") includes the data with $\psi < 90°$, and the second ("night") those with $\psi > 90°$. Section b) refers to smaller geomagnetic perturbations (maximum $\bar{K}_p < 5$), while Section c) refers to perturbations in which $\bar{K}_p$ exceeded the value of 5.

An inspection of Section b) would seem to indicate the possibility that for smaller perturbations $\Delta T/\Delta\bar{K}_p$ is a little larger in the nighttime. This result, however, is not confirmed by the larger perturbations in Section c) for which the trend is in the opposite direction, although

nonsignificant judging from the large standard deviations, which reflect the scarcity of data. Altogether we can say that if there is a difference between nighttime and daytime values of $\Delta T/\overline{\Delta K}_p$, this difference is small and cannot be determined from the observations.

From Table 4, Section a), we find that at low and middle latitudes the mean value of $\Delta T/\overline{\Delta K}_p$ in the range $0 < K_p < 5$ is 28.°3, and we can assume that in that range the relation between ΔT and K_p is close to linear. For larger perturbations the linearity of the relation breaks down, and according to previous investigations (Jacchia and Slowey, 1964a), we should approach the condition $dT/da_p = 1.°0$. The formula

$$\Delta T = 28° K_p + 0.°03 \exp (K_p) \qquad (1)$$

represents these conditions in a satisfactory manner. The alternate formula

$$\Delta T = 1.°0 a_p + 100° [1 - \exp (-0.08 a_p)] \qquad (2)$$

is almost exactly equivalent to it. Values of ΔT as a function of K_p, computed with equation (1), are given in Table 5; the values of a_p corresponding to the K_p argument can be found in the second column.

At higher latitudes ΔT should be, on the average, somewhat greater than the value given by equation (1) or (2), although a quantitative relation for the latitude dependence cannot be given on the basis of the present data. All we can say is that for latitudes above 55° Table 4, Section a), gives values of $\Delta T/\overline{\Delta K}_p$ that are systematically larger than those for

Table 5. Temperature increment as a function of geomagnetic indices.

K_p	a_p	ΔT	K_p	a_p	ΔT
0_0	0	0°	5-	39	134
0+	2	9	5_0	48	145
1-	3	19	5+	56	156
1_0	4	28	6-	67	167
1+	5	37	6_0	80	180
2-	6	47	6+	94	194
2_0	7	56	7-	111	210
2+	9	66	7_0	132	229
3-	12	75	7+	154	251
3_0	15	85	8-	179	279
3+	18	94	8_0	207	313
4-	22	104	8+	236	358
4_0	27	114	9-	300	417
4+	32	124	9_0	400	495

latitudes below 55° — by 14 percent when $K_p < 5$, and by 24 percent when $K_p \geq 5$. The very large standard deviation of $\Delta T/\overline{\Delta K}_p$ at high latitudes, when $K_p \geq 5$, may indicate that the enhancement of the atmospheric heating in the auroral zones is different for different magnetic storms. The value of 4 or 5 for the enhancement factor in two magnetic storms (MJD 38060.2 and 38070.2) given in the preliminary announcement of the effect (Jacchia and Slowey, 1964b) was somewhat overestimated. Judging from Table 2, the factor was in the neighborhood of 2, and this value must be considered as a likely upper limit for the enhancement factor, since it does not seem to be substantially exceeded in other magnetic storms.

4. REFERENCES

DE VRIES, L. L., FRIDAY, E. W., AND JONES, L. C.

1966. Analysis of data deduced from low-altitude, high resolution satellite tracking data. Paper presented at the COSPAR 7th International Space Science Symposium, Vienna, May.

JACCHIA, L. G.

1959. Corpuscular radiation and the acceleration of artificial satellites. Nature, vol. 183, pp. 1662-1663.

1964. Static diffusion models of the upper atmosphere with empirical temperature profiles. Smithsonian Astrophys. Obs. Spec. Rep. No. 170., 53 pp., December; also published in Smithsonian Contr. to Astrophys., vol. 8, no. 9, pp. 215-257., 1965.

JACCHIA, L. G., AND SLOWEY, J.

1964a. An analysis of the atmospheric drag of the Explorer IX satellite from precisely reduced photographic observations. In Space Research IV, ed. by P. Müller, pp. 257-270. North-Holland Publ. Co., Amsterdam.

1964b. Atmospheric heating in the auroral zones: a preliminary analysis of the atmospheric drag of the Injun 3 satellite. Journ. Geophys. Res., vol. 69, pp. 905-910.

1964c. Temperature variations in the upper atmosphere during geomagnetically quiet intervals. Journ. Geophys. Res., vol. 69, pp. 4145-4148.

NEWTON, G., HOROWITZ, R., AND PRIESTER, W.

1964. Atmospheric densities from Explorer 17 density gages and a comparison with satellite drag data. Journ. Geophys. Res., vol. 69, pp. 4690-4692.

ROEMER, M.

1966. Atmospheric densities and temperatures from precisely reduced observations of the Explorer IX satellite. Smithsonian Astrophys. Obs. Spec. Rep. No. 199, 82 pp.